Int. J. Heat Mass Transfer. Vol. 36, No. 4, pp. 1113–1124, 1993
Printed in Great Britain

0017-9310/93 $6.00 + 0.00
Pergamon Press Ltd

Specific features of mass transfer of discrete microparticles in the process of metallic target treatment with a powder flux

S. K. ANDILEVKO, V. A. SHILKIN and S. M. USHERENKO
Byelorussian Powder Metallurgy Association, Minsk, 220600, Belarus

and

G. S. ROMANOV
A. V. Luikov Heat and Mass Transfer Institute, Minsk, 220072, Belarus

(*Received* 17 *October* 1991)

Abstract—This paper is concerned with the problem of superdeep penetration which takes place under the conditions of metallic target treatment with a powder flux. It contains general results of experimental and theoretical investigations of the process.

INTRODUCTION

THE PROCESSES accompanying high-speed collisions represent a specific sphere of high-speed interaction, the understanding of which requires pursuance of research in the fields of solid-state mechanics, hydrodynamics, and shock-wave and high-pressure physics. In recent times this sphere of research has again attracted much attention due to the development of new technologies based on the effects of high-speed collisions and the necessity to provide dust and meteorite protection for flying and space vehicles.

The earlier studies were concerned mainly with collisions of macrobodies, which are understood to refer to the objects with characteristic dimensions exceeding 10^{-4} m. Macrobodies were used to study the effects of various high-energy interaction parameters on the characteristics of craters (channels) formed under collisions.

In refs. [1, 2] the influence of speed (specific interaction energy), angle of encounter, strength, heat and other parameters of bodies on the processes of their collision was considered. According to ref. [1], the most important collisional parameter in solids is the initial speed of a particle, because it determines the specific energy which, in turn, is of critical importance for the character of interaction. The whole experimental range of interaction speeds ($\leqslant 90$ km s^{-1}) can be conventionally divided into six intervals [1], differing substantially from each other in the character of physical processes proceeding in them:

(1) The speed of collision $U_0 \leqslant 50$ m s^{-1} (the characteristic rate of deformation $\dot{\varepsilon} \simeq 10^0$ s^{-1}). The interactions of bodies are determined by their elastic characteristics, except for very plastic objects (plasticine, resin and so on).

(2) 50 m s^{-1} $< U_0 \leqslant 500$ m s^{-1}; $\dot{\varepsilon} \simeq 10^2$ s^{-1}. The collisional process is accompanied by plastic deformation of a particle and of a target. The relative depth of penetration (RDP) never exceeds a few initial particle sizes (units).

(3) 0.5 km s^{-1} $< U_0 \leqslant 1.0$ km s^{-1}; $\dot{\varepsilon} \simeq 10^4$ s^{-1}. In this range of speeds a particle and a target show their viscosity properties. Here and hereafter, the term 'particle' denotes one of the bodies experiencing collisions, the mass of which is much smaller than the mass of the other object, i.e. a target. The material strength characteristics also exert a pronounced effect on the results of collisions. The shape of the crater obtained in this case depends strongly on the shape and the properties of the particle. When colliding bodies are brittle [2], a crater is rather like a shallow dent with a highly branched network of cracks and spallings. Usually, the penetration of a rigid particle into a plastic target culminates in the formation of a narrow funnel (channel) which is extended into the target and the depth of which never exceeds 3–4 units.

(4) 1.0 km s^{-1} $< U_0 \leqslant 3.0$ km s^{-1}; $\dot{\varepsilon} \simeq 10^6$ s^{-1}. Near the surface of contact, colliding bodies act like fluids, the compressibility of which can be neglected. As a rule, the stresses generated by shock waves in a particle and a target exceed their yield stress. Here, the impact of a particle produces a crater with a hemispherical bottom at the end of a cylindrical channel. The crater is surrounded by a circular ledge formed by the target material displaced from inside the hole. In this case the RDP does not exceed 7. The crater depth to diameter ratio is $N \leqslant 6$. The channel diam-

NOMENCLATURE

a^2	thermal diffusivity
$\bar{c}$, c	specific heat and sound velocity of target, respectively
d	diameter of a particle
E	enthalpy of weakened substance flow
F_g	force acting on rear side of particle
h_*	depth of particle penetration into target
H	hardness
l	height of cylindrical particle
L	latent heat of melting
M	mass of a particle
N	ratio of channel diameter to its depth
p	stress
q	heat flux
S	area
t	time
$\mathcal{W}$, W, U	velocities of weakened substance flow around a particle
V_1, V_2	speeds of overtaking stream and convergence point, respectively.

Greek symbols

α	converging angle of channel
ε	specific energy
$\dot{\varepsilon}$	rate of deformation
λ	thermal conductivity
$\bar{\lambda}$	thickness of slip plane of target
μ	viscosity
ρ	density
τ	time interval.

Subscripts

d	parameters of deformation
f	flux parameters
i	parameters of single pulse
k	critical parameters
m	parameters of melting
p	parameters of particle
R	parameters of relaxation
t	parameters of target
1	parameters of overtaking stream.

eter in this case is always greater than the initial diameter of the particle.

(5) 3.0 km $s^{-1} < U_0 \leqslant 12.0$ km s^{-1}; $\dot{\varepsilon} \simeq 10^8$ s^{-1}. Solid bodies behave like fluids, the compressibility of which exerts a significant effect on the process of collision. The fraction of the interaction energy spent on heating the bodies and on their thermal destruction increases considerably. The crater is a lune surrounded by a shaft of the melted target substance. In this case the RDP does not exceed 8–10 units and the value of N decreases significantly. The crater diameter is much greater than the initial particle diameter.

(6) $U_0 > 12.0$ km s^{-1}; $\dot{\varepsilon} \geqslant 10^8$ s^{-1}. The process of 'particle–target' collision is accompanied by explosive energy release and evaporation. The shape of the crater is close to hemispherical, $N \simeq 0.5$ [2]. In this range of speeds, the fraction of energy spent on thermal destruction of bodies increases drastically. Generally, the particle disappears. The RDP is not higher than 15.

Based on the studies of processes taking place under macrocollisions, the authors of refs. [3, 4], who investigated the problems of meteorite protection of spacecraft, came to the conclusion that most hazardous for these vehicles are the erosion and deterioration (wear) of surfaces. The penetration of microparticles through the shields ($h \leqslant 10^{-4}$ m) over the speed range up to 15 km s^{-1} was considered to be highly improbable. According to estimates [3], only one hole may appear on a 6-mm-thick protecting cover over the area of 100 mm^2 for the period of one year. It was supposed that such protection could be pierced only by macrometeorites, the encounter with which in space is a relatively unlikely event.

However, the studies of collisions of solid bodies with clusters of particles have yielded results which slightly differ from those discussed above. For instance, when metal targets were treated by tungsten and zirconium alloy clusters of particles having fractions of 80–100 and 85–100 μm, respectively, it was demonstrated [5] that for a speed of about 1.5 km s^{-1} the RDP should be 2–6 times higher than the maximum possible value from the viewpoint of the available ballistic methods of calculation [6]. Trying to explain this anomalous behaviour [5], the authors assumed that the particles, the diameters of which do not exceed 200 μm, move along the boundaries of the grains where their energy expenditures for overcoming the resistance forces could be somewhat lower. It was noted therewith that the diameters of craters detected on the target surface turned out to be much smaller than the diameters of initial particles. This allowed an assumption that the penetration of a particle into the surface was followed by partial or complete collapse of the channel. Should the process of the formation of craters be subdivided, according to ref. [6], into four principal stages—unsteady state, plastic deformation of a target on direct contact with a particle, afterflow when enlargement of the cavity takes place by inertia after direct contact of the particle with a target and channel compression, under residual elastic stresses or under the stress field formed in the target from the outside—it should be emphasized that during the treatment of a metal target by a cluster (or stream) of particles the last stage gains

in importance. This results in a partial or complete collapse of the cavity.

It should be noted that in all the earlier works where, just as in ref. [5], anomalous behaviour in the data on collisions of metallic bodies with clusters of particles was observed, the results obtained were not always stable. Only at the end of the 1970s to the beginning of the 1980s did stability appear in the results on the superdeep penetration of microparticles (down to 10^4 units) [7, 8]. This effect has been given the name 'superdeep penetration' (SDP) or 'superdeep mass transfer'.

When this effect is realized, the structure and the properties (physical, chemical, thermal, mechanical, etc.) of a target undergo significant variation. It should be noted that the existence of the effect is determined in this case not only by the loading conditions (cluster parameters), but also by the properties of the target material. Significant dependence of the SDP on the size of particles has been revealed. The SDP effect was not registered in direct experiments on loading a metal target by a flux of particles with characteristic sizes $d > 10^{-4}$ m, while for powder with the sizes of particles below 100 μm this effect is observed regularly.

The present paper will consider the specific features of the structure and mechanical properties of targets treated with a flux of powder particles under the conditions of superdeep mass transfer, as well as some other problems of SDP modelling.

EXPERIMENTAL METHODS

Experiments with the use of a scanning electron microscope (SEM)

The procedure of preparing samples for SEM examination included cutting, mechanical polishing with the use of aluminium- and chromium oxide-based pastes, and chemical etching in a 10% alcoholic solution of nitric acid for 4 min. Before examination, the prepared samples were placed into a bath with acetone through which ultrasound was then passed. The microsections were examined with the aid of SEM 'Nanolab-7'. The chemical composition of the observed structural components was determined with the use of an attachment for an X-ray microspectral analyzer.

Layer-by-layer chemical analysis

Chemical analysis was carried out by the atomic absorption spectrometry method. Solutions of the studied materials in acid mixtures were analyzed layer-by-layer with the use of a spectrophotometer.

Examination by transmission electron microscopy (TEM)

Samples of thin foil (0.3–0.4 mm) were cut out from the specimens by the electric-spark method at a specified depth in the direction normal to the particle flux direction to the target. The samples were then lapped and polished by abrasive disks and pastes to a thickness of 50–70 μm and then polished electrochemically. The plate thus produced was studied by TEM.

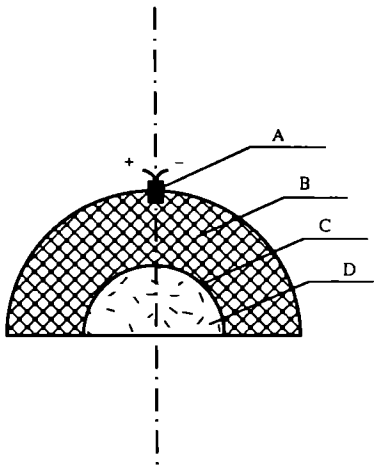

FIG. 1. Schematic diagram of an explosive accelerator: A, electric detonator; B, charge of explosive; C, container envelope; D, powder.

Forming a flux of powder particles

Stability in the observation of the SDP effect was achieved only in the conditions of loading a metallic target by a particle flux formed by means of an explosive accelerator, a schematic of which is shown in Fig. 1 [9]. For the majority of materials the average speed of the flux amounts to about 1–3 km s^{-1} and the mean density to about 0.5–6 g cm^{-3}. The flux consists of discrete particles ($d < 10^{-4}$ m). Its interaction with a target is unsteady and pulsed in character.

EXPERIMENTS

Detection of the remains of a single particle and examination of the crater formed by it in a target generally presents no special problems. The situation is different in the case of superdeep penetration of powder particles. Cavities of various shapes and depths appear on the surface of a target as well as sintered conglomerates of particles, which can usually be easily separated. The irregularities can be eliminated by mechanically removing a 1–2 mm thick surface layer. The depth of penetration was calculated from the 'clean' surface. No cavities have been detected on the surface even when examining by SEM with magnifications of up to × 1000. Thus, to produce proof of the penetration of microparticles into a target by means of direct observations of unetched microsections is difficult due to the small sizes of particles ($d < 100$ μm) and the properties of the channel structure. For this reason, numerous special tests were

run for demonstrating the effect of superdeep mass transfer. Targets made from different materials (copper, aluminium, titanium, iron and steels with different contents of carbon and addition agents) were investigated. The basic requirements imposed on powders were:

(1) their composition should not involve chemical elements contained in the target;

(2) the size of powder particles should not exceed 100 μm.

The evidence that the material of impinging particles is present in a target was obtained by using the methods of layer-by-layer chemical and X-ray microspectral analysis. Chemical etching enabled isolation of impinging particles from the target structure (Figs. 2(a), (b)).

While penetrating into the target, the powder particles form there a network of microchannels in the zone of which intensive plastic deformation and interaction of particles with the walls of the channels are observed.

Due to the difference in the properties of the target and channel material, there appears to be the possi-

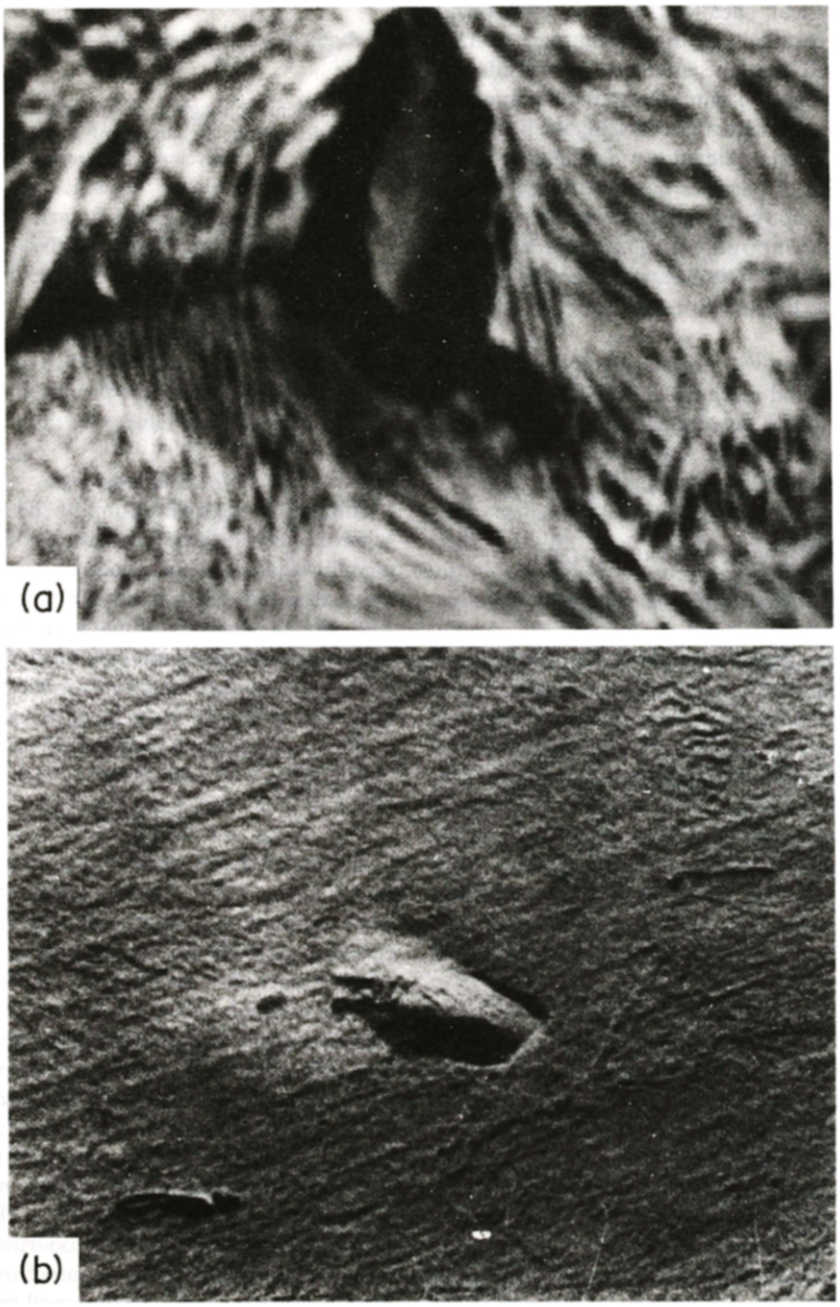

FIG. 2. Structure of steel with 0.1% carbon (×2500) at a depth of 2 mm after treatment with a mixture of powders: (a) iron + tungsten; (b) nickel + tungsten.

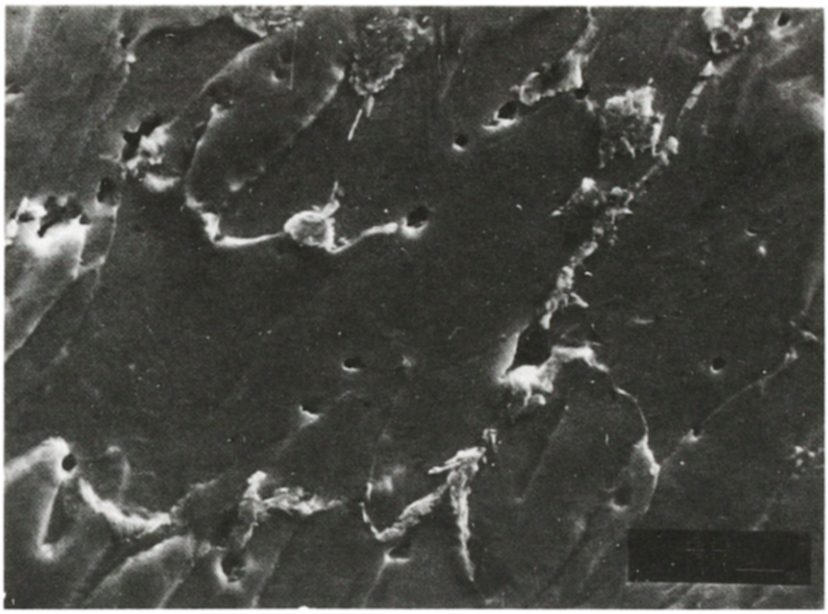

FIG. 3. Structure of steel with 0.1% carbon (×2500) at a depth of 2 mm after treatment with titanium diboride.

bility of observing the channels on the microsections that were chemically etched. On transverse microsections (i.e. those the observation plane of which is perpendicular to the direction of powder flow injection) the etched channels are seen as roundish voids (Fig. 3). When the microsection plane coincides with the particles, the latter could be observed. In Fig. 4 the structure of steel with 0.1% of carbon at a depth of 5 mm from the surface treated by a flux of titanium powder is shown. The detected particle contains about 80% (by mass) titanium, the rest being iron and impurities. The composition of the particle was identified with the aid of an X-ray spectral microanalyzer.

Investigation of the target structure on microsections, the observation plane of which coincides with the direction of the penetration of a powder flux, makes it possible to follow the path of the particles in the target material. In order to more clearly reveal the channels, the target was treated with fluxes of copper (0.5–5.0 μm) or plumbum (36–32 μm) particles which, together with an etchant, form almost indissolvable compounds. Figure 5 shows the structure of steel containing 0.45% carbon which was treated by copper powder (to a depth of 2.4 mm). A stretch of the channel is observed to be coincident with the microsectional plane. At the cross-section the channels are divided into two zones. The central zone is darker, and is surrounded by a white zone of thermal effect hardly susceptible to etching. The relative penetration depth was approximately equal to 6.9×10^2.

In the carbon steel treated by a flux of plumbum powder, channels were detected in which the zones of entry and the remains of the particle were easily discernible (Fig. 6). Ahead of the particle, a tapered cavity could be observed. The ratio of the maximum depth at which plumbum inclusions were detected to the initial particle size amounted to about 1.95×10^2.

Of indubitable interest is the fact that moving particles intersect the boundaries of the grains (Figs. 5 and 7). This implies that the effect of grain boundaries on the particle path in the material of the target is insignificant.

Numerous experiments conducted on steels with different contents of carbon and different structures of grained and sliced perlite have made it possible to observe a strong effect of superhard inclusions (ferric carbides) on the penetration process. The greater the amount of inclusions in the initial structure, the more intricate is the path of the penetrating particle. It resembles vibrations in different planes, with a certain direction of motion being preserved. In highly-doped steels that contain about 20% (by mass) carbide phase, traces of particle collisions with carbides have been detected (Fig. 8).

Taking into account the possible effect of diffusion processes on the formation of the channel structure, some amount of work was devoted to the study of iron treated with nickel, silicone and tungsten powders with particles of sizes from 5 to 8 μm. These elements have substantially different atomic radii and, consequently, different diffusion powers. Inspection of iron at depths down to 5 mm has shown that the zones containing the introduced material are indentical in all three cases. The size of these zones is commensurable with the diameter of the particles. As an example, Fig. 9 shows the structure of iron treated with tungsten to a depth of about 4 mm. The points mark the places of X-ray microspectral analysis.

Under certain conditions of the collisions of particles with a target, the formation of the structure of

fibre-armoured material was observed in steel. Figure 10 depicts the structure of steel with 0.45% carbon treated with niobates: the activated matrix zone had been etched so that the compounds of doping elements with the target material were found in the centres of the channels.

The differences in etching of the channels and matrix material are indirect statements to the fact that there is a severe plastic deformation localized in the channel zones. The existence of such a deformation was also demonstrated by a direct experiment with iron treated by a flux of silicone nitride particles, with its structure then being examined by transition electron microscopy. As illustrated by Figs. 11(a)–(d), the imperfection degree of the target material decreases with an increase in the distance from Si_3N_4 particles, while close to the centre of the observation zone the material can be regarded as being devoid of any structural order. At a distance of 2–3 particle diameters, this degree of imperfection does not differ from the initial state.

In addition to the structural study, quantitative analysis of the effect of particle sizes on the channel diameter, density of channelling and the structure porosity of tool steel was performed. The powders used were titanium diboride particles with sizes under 3, 10–14 and 40–50 μm. Investigations were carried out at four different depths (0.5, 2.5, 5.5 and 8.0 mm) characteristic for this set of experiments. It was found that variations in the structure parameters with the section depth for a given powder fraction are of complex non-linear character. The channel diameters can increase with depth, pointing to the fact of the non-uniform loss of mass by particles in the process of penetration. The density of channelling at a depth of about 5.5 mm varies from 10^2 to 10^3 mm^{-2} for different pairs of materials in a powder–target system.

In summary, it can be noted that the effect of superdeep mass transfer is characterized by the following features:

(1) SDP is observed only in conditions of target loading by a flux of particles with an adequate density ($\rho \simeq 10^3$ kg m^{-3}). Penetration of single particles has not been observed.

(2) The characteristic sizes of interacting particles should not exceed a certain critical value ($d_k \simeq 10^{-4}$ m). The experiments conducted to detect SDP for the particles having $d > d_k$ have given negative results (superdeep mass transfer was non-existent).

(3) The channels formed by particles moving in the target material collapse and can be detected only after additional treatment of microsections (etching in a 10% solution of nitric acid). The sizes of the channels detected after etching do not exceed the initial sizes of the penetrating particles.

(4) The target material in the area near the channels experiences severe plastic deformations in the process of the penetration of particles, and this determines its fast solubility in acid as compared with the initial material.

Based on the foregoing, it can be noted that a theoretical description of the motion of a single particle with realization of the SDP effect must take into account the collective effect of particles on the surface of a metal target.

THEORY

The equation of motion of an individual particle in the target material under the conditions of plastic interaction can be written as follows [10]:

FIG. 4. Structure of steel with 0.1% carbon (× 5000) at a depth of 5 mm after treatment with titanium powder.

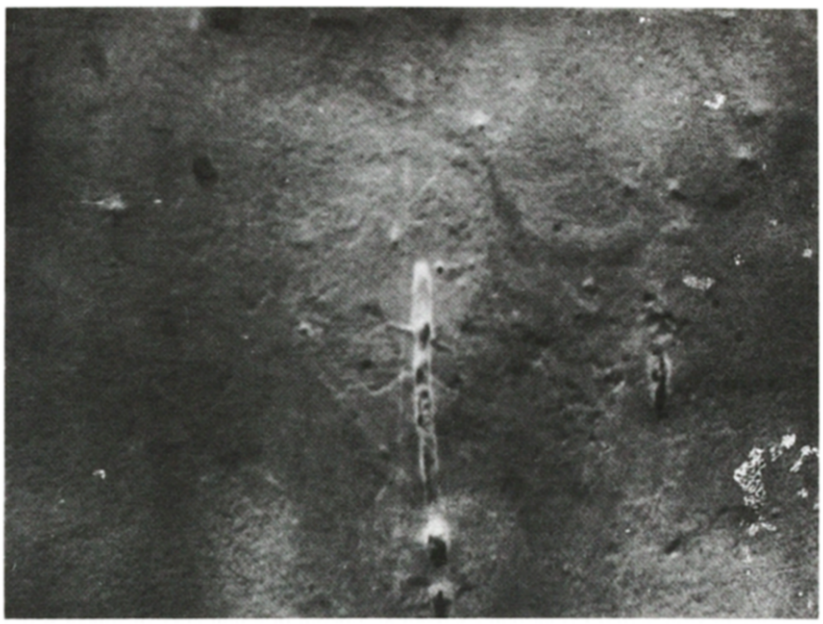

FIG. 5. Structure of steel with 0.45% carbon (×2000) at a depth of 7 mm after treatment with copper powder.

$$M(\mathrm{d}U/\mathrm{d}t) = -H_t S - pS - \rho_t U^2 S/2 - \rho_t \mu_t U/d + F_g \quad (1)$$

where H_t, ρ_t and μ_t are the hardness, density and kinematic viscosity of the target material, respectively; U, S and d are the instantaneous speed, frontal area and the characteristic size of the particle. To be explicit, it is assumed that the particle has a cylindrical form with $d \simeq l$, where l is the height of the cylinder which moves along its symmetry axis; F_g is the force acting on the rear side of the particle. For a single particle $F_g = 0$.

Integrating equation (1) ($\mu_t \simeq 10^{-2}\ \mathrm{m^2\,s^{-1}}$; $H_t \simeq 1$–$7\ \mathrm{GPa}$ [10, 11]; $\rho_t \simeq 8 \times 10^3\ \mathrm{kg\,m^{-3}}$; $U_0 \simeq 2\ \mathrm{km\,s^{-1}}$; $d \simeq 10^{-5}\ \mathrm{m}$), subject to the conditions

$$U(t = 0) = U_0 \quad \text{and} \quad U(x = h_*) = 0 \quad (2)$$

(where U_0 is the initial collision rate and h_* is the

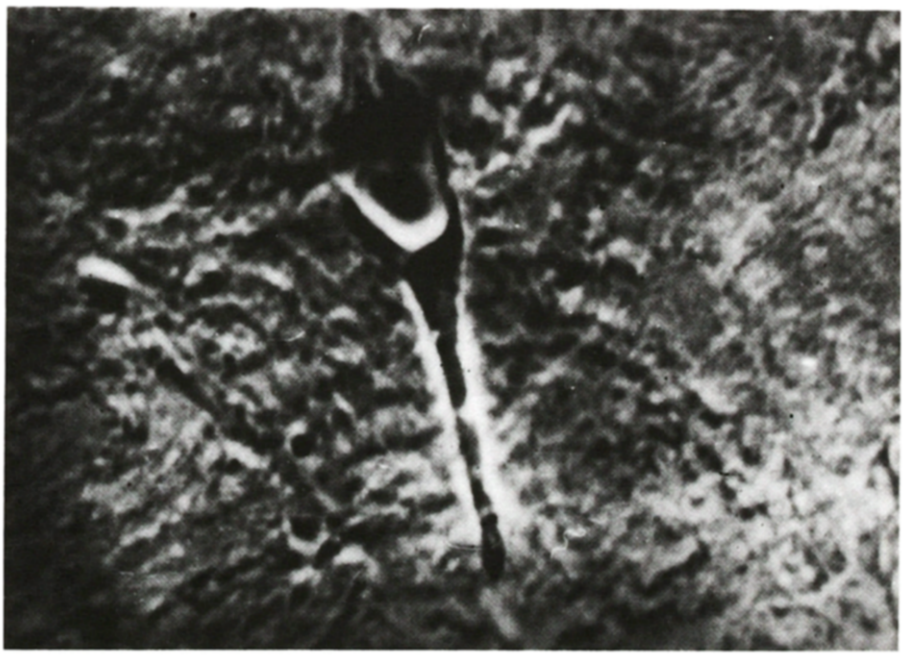

FIG. 6. Structure of steel with 0.45% carbon (×5000) at a depth of 6 mm after treatment with plumbum powder.

FIG. 7. Structure of steel with 0.1% carbon (× 1000) at a depth of 4 mm after treatment with titanium diboride powder.

penetration depth), give $h_* \leqslant l \simeq d$. Such a small value of h_* is due to the large energy losses in overcoming the strength and viscosity components of the resistance force.

Consequently, there should exist a certain mechanism which is responsible for the loss of strength by the target material and for a marked decrease in the H_t and μ_t values. In the authors' opinion, such a mechanism really exists and can be revealed even on brief examination of the processes taking place in a target loaded by a flux of particles.

When a target is loaded by a high-density ($\rho_f \simeq 10^3$ kg m^{-3}, $U_f \simeq 1$–3 km s^{-1}) flux of particles ($d \simeq 10$ μm) lasting $\tau \simeq (2$–$7) \times 10^{-5}$ s [12], a variable pressure field originates in it in which compression pulses alternate with the pulses of partial off-loading. The duration of separate pulses of this type is of the order of the characteristic time of the 'particle–target' interaction ($\tau \simeq \tau_d \simeq \dot{\varepsilon}^{-1} = d/U \simeq 10^{-8}$ s); the intensity is defined as

$$p \simeq 0.3\rho_t c U_t \tag{3}$$

where c is the speed of sound in the target material. When $c \simeq 5$ km s^{-1}, the intensity is $p \simeq 1$–5 GPa. The

FIG. 8. Structure of high-speed steel with 6% tungsten (× 1000) at a depth of 2 mm after treatment with nickel powder.

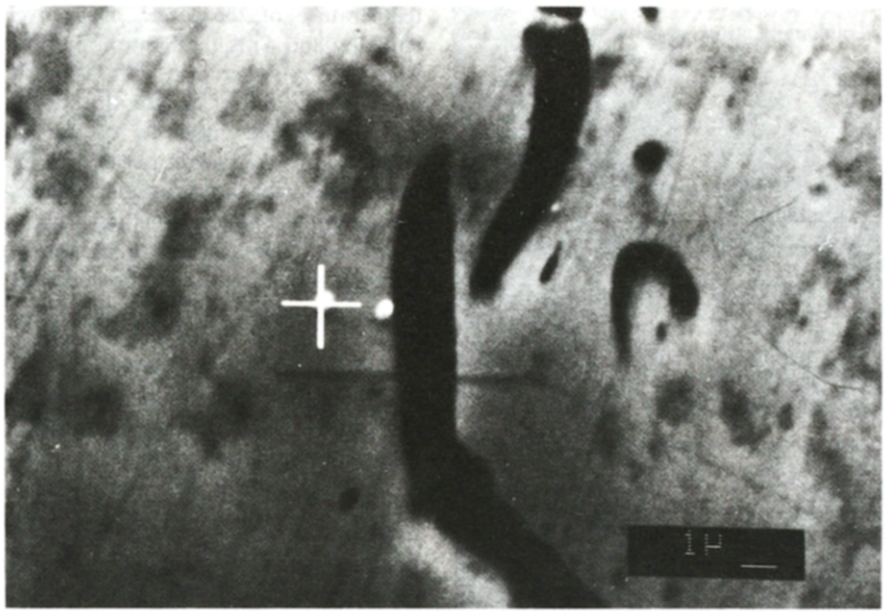

FIG. 9. Structure of steel (× 1000) at a depth of 4 mm after treatment with tungsten powder.

specific energy imparted by such a pulse to the crystal lattice ε_i amounts to 10^4 J kg^{-1} which corresponds to warming-up by $\Delta T \simeq \varepsilon_i/\bar{c} \simeq 10$–$20$ K. At the same time, the number of such pulses is approximately equal to $(2$–$7) \times 10^3$. With allowance for heat removal, the specific energy of the lattice is increased by about 10^6 J kg^{-1} under the influence of pressure field generated in the target by the flux. This increase is comparable in magnitude with the specific energy required for melting a unit mass of a target, $\varepsilon_m \simeq \bar{c}T_m + L_m$, where T_m, L_m and $\bar{c}$ are the melting temperature, latent heat of melting and specific heat of the target, respectively. In the area comparable with the characteristic dimensions of the flux ($L \simeq 0.1$ m), the target material is heated up to the temperature $T \simeq T_m$ and exhibits instability when even an insignificant effect of some object would suffice to completely destroy all the crystalline bonds in the target material. This object can be a penetrating particle whose specific energy of interaction with the target material is equal to $\varepsilon_p \simeq U^2/2 \simeq 10^5$–$10^6$ J kg^{-1}. The characteristic time of interaction τ_d is comparable with $\tau_m \simeq (2/3)\lambda\rho_t\bar{c}(T_m - T_0)^2/q^2$, where τ_m is the time required for heating the target material up to the melting temperature at the heat flux $q = St \cdot EU$; λ and T_0 are the thermal conductivity and the initial

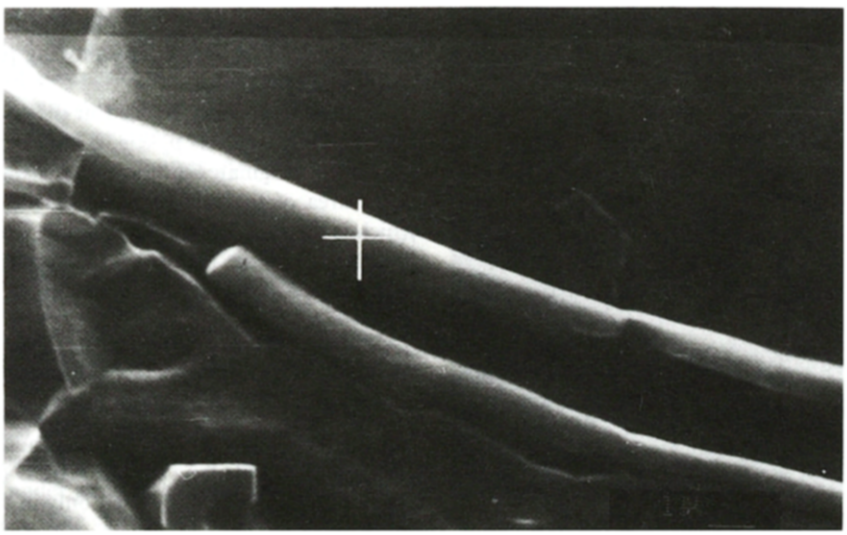

FIG. 10. Structure of steel with 0.45% carbon at a depth of 10 mm after treatment with niobium compound powder.

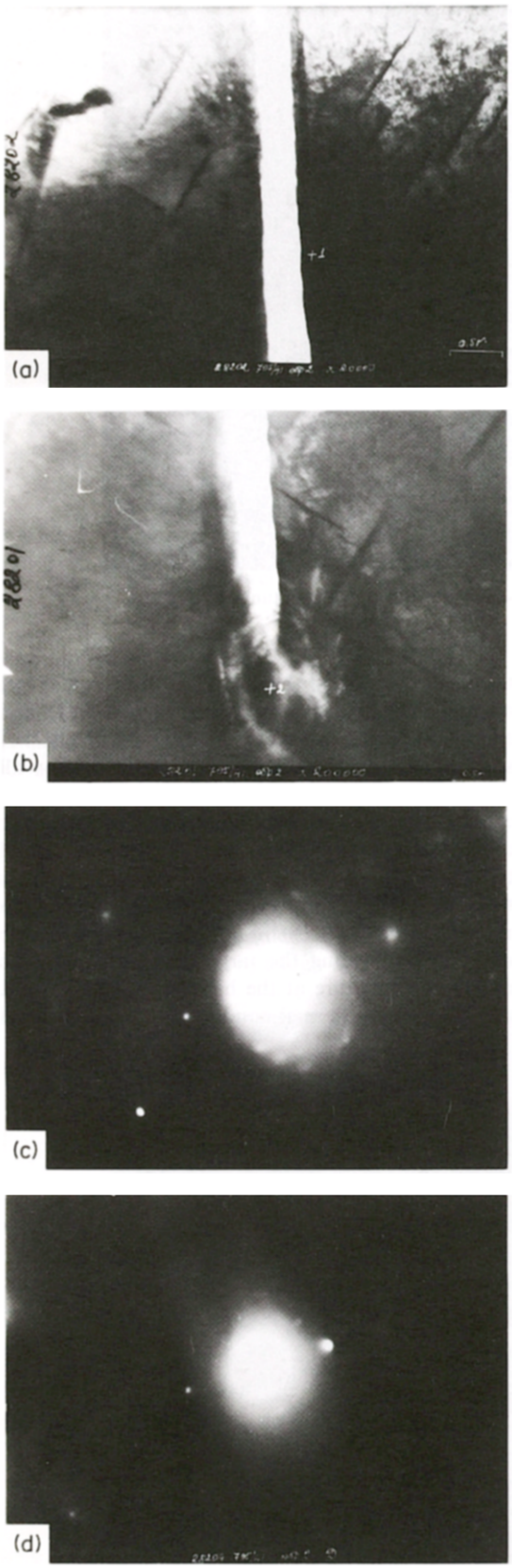

FIG. 11. Structure of iron (×13500) at a depth of 7 mm after treatment with silicone nitride powder: (a), (b) thin structure; (c), (d) electron diffraction patterns of the zones +1(b)+2(a).

temperature of the target, respectively; E is the enthalpy and St is the Stanton number. In the case when $\tau_U \leqslant \tau_R$ (where $\tau_R \simeq \bar{\lambda}^2/a^2$ is the time of thermal relaxation, $\bar{\lambda}$ and a^2 are the thickness of slip planes and the thermal diffusivity of the target material, respectively), the energy released in 'particle–target' interaction is localized near the contact zone, causing the unhardening or even melting of the target material in this area. The viscosity μ_t and strength H_t of the material in this area are comparable with the viscosity μ_m and strength H_m of the melt ($\mu_m \simeq 10^{-5}$ m^2 s^{-1}, $H_m = 0$ [13]). The Reynolds number is $Re = dU/\mu_m \simeq 10^3$. Since $Re \gg 1$ and $U_f \leqslant c$, the motion of the particle in the target can be considered as motion in an inviscid incompressible liquid. In this case the equation of motion is

$$M(\mathrm{d}U/\mathrm{d}t) = -pS - \rho_t U^2 S/2 + F_g. \qquad (4)$$

However, in the case of penetration of individual particles ($F_g = 0$), direct integration of equation (4) under conditions (2) gives the maximum penetration depth $h_* \leqslant 50d$. For penetration to a depth of about 10^{-3}–10^{-4}, a particle should have at least 10^2–10^3 times larger energy.

The only energy source in this case is the potential energy of the pressure field generated in the target by a flux of particles.

This energy should be transferred to the particle gradually during the entire process of penetration, since a single energy increase (and a corresponding 10–20 fold increase in velocity) would have resulted in an uncontrollable growth of the specific energy of the thermal interaction between the particle and the target, as a consequence of which the process of thermal destruction of the particle and the target becomes more likely [1].

The postulated mechanism involved in the transfer of energy accumulated by a powder flux in the crystalline lattice of the target can be established by considering the processes taking place during the closure of the channel formed by the moving particle in the target material.

Really, the pressure formed in the channel behind the moving particle is $p_r \ll p$. A difference of forces, $f_c \simeq \Delta p S_c$, originates on the channel walls (where S_c is the area of the side surface element, $\Delta p = p - p_r$) which is directed toward the channel axis. Under the influence of f_c the channel is converging to the axis with a speed $W = W(\Delta p)$. The angle of convergence is

$$\alpha = \arccos\,[U/(U^2 + W^2)^{1/2}]. \qquad (5)$$

The speed of channel convergence can be determined from the conservation condition for the Bernoulli integral along the line ABCD (Fig. 12). The Bernoulli theorem can be used only in the case when the time of channel collapse $\tau_x \ll \tau_h$ (where τ_h is the time of particle motion in a target), because in this case the particle velocity varies insignificantly. The

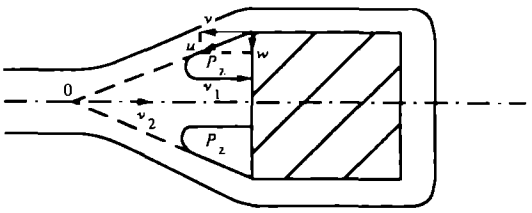

FIG. 12. Schematic of flow of weakened substance around a particle under SDP conditions.

motion over this time interval can be regarded as stationary. Then

$$\rho_t \mathscr{U}^2/2 = \Delta p + \rho_t U^2/2 \quad \text{and} \quad \mathscr{U}^2 = U^2(1+2\Delta p/\rho_t U^2) \tag{6}$$

$$\mathscr{U}^2 = U^2 + W^2 \quad \text{and} \quad W = (2\Delta p/\rho_t)^{1/2}. \tag{7}$$

When the convergence angle α (Fig. 12) exceeds a certain critical value α_k (for steel and aluminium $\alpha_k \simeq 20$–30 [14]), the flow originates at the point of convergence O (an overtaking stream, OS) which propagates in the direction of particle motion. The conditions of formation and motion of the overtaking stream are similar to those of a cumulative stream [15]. Its velocity in the coordinate system moving with the point O is $V_1 = \mathscr{U}$. The velocity of the point O in the laboratory system is $V_2 = \mathscr{U}/\cos\alpha = U(1+2\Delta p/\rho_t U^2)$; consequently, the velocity of the overtaking stream in the laboratory coordinate system is

$$V = V_1 + V_2 = U(1+\gamma)^{1/2}[1+(1+\gamma)^{1/2}] \tag{8}$$

where $\gamma = 2\Delta p/\rho_t U^2$. Since $V > U$, the overtaking stream rapidly (in the time $\tau_1 \simeq d/\mathscr{U} \simeq 10^{-9}$ s) overtakes the particle and, retarding on its trailing side, transfers a part of its energy. The force acting on the trailing side of the particle is given by

$$F_g = S_1\rho_t(V-U)^2 + pS_1 + p_z(S-S_1)$$

where S_1 is the area of the spot of contact between the particle and the overtaking stream. The velocity of the point of contact O is $V_2 > \mathscr{U}$. Consequently, after a certain period of time ($\tau_2 \simeq 10^{-8}$–10^{-9} s) the point of contact also emerges onto the trailing side of the particle. The cavity collapses. As this takes place, $S_1 \to S$, $p_z \to p$, $V \to 2U$ and

$$F_g = S\rho_t U^2/2 + pS. \tag{9}$$

The substitution of F_g into equation (4) yields $M(\mathrm{d}U/\mathrm{d}t) = 0$. Since $M \neq 0$, then $U = U_* = \text{const}$. This means that from the instant the channel closes completely and so long as the pressure p exists in the target, the particle will move uniformly. The particle velocity is equal to that reached at the start of uniform motion and can be determined from the integration equation (4) under additional conditions $F_g = 0$ and $U(t = \tau_x) = U_*$. The calculations performed made it possible to determine that at $p = 2$–5 GPa, $\rho_t \simeq 7830$ kg m^{-3}, $d = 10$ μm, $U_0 = 1500$ m s^{-1} and $\rho_p = 8900$ kg m^{-3}, the velocity $U_* \simeq 800$–1200 m s^{-1}. In this case the ultimate depth of the particle penetration is

$$h_* \simeq U_*\tau_0 \simeq 0.016\text{–}0.084 \text{ m}$$

or $h_*/d = 1600$–8400, in accordance with the experimental results.

The model suggested has been developed for the simplest case of $p = \text{const}$. However, usually $p = p(r, t)$, where r is the radial coordinate from the stream axis. In this case, the particle motion can be composed of a large number of regions of steady (uniform) and unsteady motion. The full depth of penetration can be determined by their successive summation.

It has been found at the beginning of this section that the characteristic time of the particle interaction with a target τ_d should not exceed the time of thermal relaxation τ_R, since otherwise it would be impossible to localize the amount of energy sufficient for unhardening the material in the zone of interaction. Here, the motion of the characteristic time of interaction includes not only τ_d, but also $\tau_{cx} \simeq d/W$, i.e. the time of channel collapse. Thus, the necessary SDP condition can be written in the form of the inequality

$$\tau_{cx} + \tau_d \leqslant \tau_R$$

or after the substitution

$$d \leqslant d_k \quad \text{and} \quad d_k \simeq (\bar{\lambda}^2/a^2)(2p/\rho_t)^{1/2}(1+\gamma)^{-1} \tag{10}$$

where d_k is the critical size of the penetrating particles. For $p = 0$ (a single particle), $d_k = 0$. The penetration of single discrete particles into a metallic target by the SDP mechanism is impossible. When $p \to \infty$, d_k approaches its limiting value

$$d_k = (\bar{\lambda}^2/a^2)U_0.$$

From condition (10) it follows that the superposition of the additional pulsed pressure, synchronized with a stream directed to the target side surface, should lead to an increase in d_k and, thus, to the enlargement of the range of particles for which the SDP effect can be observed. This, in turn, should cause an increase in the number of particles entering the metal. This has been proved experimentally. When the pressure is raised by 20–30%, a 1.5–2-fold increase in the concentration of the material introduced is observed.

Another condition for the penetration is $d > d_k$ or $\cos\alpha < \cos\alpha_k$. This suggests that the pressure generated in a target by a flux should obey the condition

$$p \geqslant p_k \quad \text{and} \quad p_k = \rho_t U^2 \tan\alpha_k. \tag{11}$$

The calculations show that in the case of steel $d_k \simeq 70$–90 μm, $p_k \simeq 0.1$–1 GPa.

Summarizing the results, it should be pointed out that the assumption about the collective nature of SDP—i.e. when a larger portion of the flux, retarding on the target surface, transfers its energy to the target

material where it is accumulated in the form of the pressure-field potential energy and, under certain conditions, can be subsequently transferred to certain particles for their deeper penetration—provides an opportunity not only to explain the SDP process, but also to predict with adequate accuracy the results of its realization on variation of the loading conditions.

DISCUSSION

Based on experimental and theoretical studies of the interaction of a dense flux of microparticles with a metal target, a new physical phenomenon—superdeep penetration (mass transfer)—has been described. The special features associated with the penetration of particles into the target have been determined experimentally. An adequate physical model of the process has been developed.

In this section, some aspects connected with the technological use of SDP will be considered.

After the treatment of the target by the flux of particles and their superdeep penetration, the structure of the material undergoes substantial changes. There appear fibrous formations oriented predominantly in the direction coinciding with the powder flux direction.

The properties of new materials depend on the properties of the target material and powder introduced, on the regimes of blast loading and on the subsequent heat treatment. In the general case, a significant improvement of such mechanical characteristics as the tensile strength, wear resistance and hardness has been attained, with the impact viscosity being preserved at the initial level. Specifically, the wear resistance of high-speed steel containing 6% W and 5% Mo in the conditions of abrasive wear increases by a factor of 1.5–2.2. These changes extend over the entire depth of the item (down to 20 mm). This has enabled one to use the phenomenon of superdeep penetration (SDP) for developing new materials for the reinforcement of cutting tools of cutter-loaders and strengthening the metal-cutting swaging tools. The technology of introducing the particles of powder into the compact targets and also the recommendations on the possible use of SDP have been developed at the Byelorussian Powder Metallurgy Association.

REFERENCES

1. J. Zukas, Penetration and perforation of solids. In *Impact Dynamics*, pp. 110–158. Izd. Mir, Moscow (1985).
2. A. G. Bazilevskiy and B. A. Ivanov, Survey of the advances in the field of the mechanics of crater formation. In *Mechanics of Crater Formation on Impact and Explosion*, Ser. Mechanics, pp. 172–227. Izd. Mir, Moscow (1978).
3. T. N. Nazarova, Consideration of meteorite particle encounter with holes and piezoelectric pickups when evaluating the spatial density of the meteorite substance, *Kosmicheskiye Issledovaniya* **10**(4), 600–603 (1972).
4. Yu. S. Stepanov, Some problems of breakthrough on collision with meteorite particles, *Kosmicheskiye Issledovaniya* **3**(6), 903–916 (1965).
5. R. E. Gannon, T. S. Lashlo, K. E. Ley and S. I. Walnick, The influence of microparticle bombardment on optical properties of metals, *AIAA J.* **3**(11), 148–157 (1965).
6. N. A. Zlatin and G. I. Minin (Editors), *Ballistic Systems and their Use in Experimental Studies*. Izd. Nauka, Moscow (1974).
7. V. G. Gorobtsov, S. M. Usherenko and V. Ya. Furs, Concerning some effects of a high-speed flux in treatment of the working matter. In *Powder Metallurgy*, No. 3, pp. 8–12. Vysh. Shkola, Minsk (1979).
8. S. K. Andilevko, V. A. Shilkin and S. M. Usherenko, Introduction of metallic powders into steel. In *Treatment of Materials at High Pressures*, pp. 64–67. Izd. IPM ANUSSR, Kiev (1987).
9. S. K. Andilevko, Ye. N. Sai, G. S. Romanov and S. M. Usherenko, Motion of a particle in metal, *Fiz. Goren. Vzryva* **27**(7), 110–113 (1988).
10. V. A. Kozlov, The penetration model taking into account the viscous properties of the materials of colliding bodies, *Problemy Prochnosti* No. 3, 47–52 (1986).
11. G. V. Stepanov and V. V. Kharchenko, Specific features of the deformation of metals, *Problemy Prochnosti* No. 8, 59–64 (1985).
12. L. V. Altshuler, S. K. Andilevko, G. S. Romanov and S. M. Usherenko, About the model of superdeep penetration, *Pis'ma v Zh. Tekh. Fiz.* **15**(5), 55–57 (1989).
13. C. Smithells, *Metals Handbook*. Izd. Metalurgia, Moscow (1980) [in Russian].
14. S. A. Kinelovskiy and Yu. A. Trishin, The physical aspects of cumulation, *Fiz. Goren. Vzryva* **19**(5), 26–40 (1980).
15. M. A. Lavrentyev and B. V. Shabat, *The Problems of Hydrodynamics and Their Mathematical Models*. Izd. Nauka, Moscow (1973).